Multiscale Noise and Vibration models for a Switched Reluctance-based drivetrain for EV and HEV

Koen De Langhe - Senior Product Line Manager Noise and Vibration
Koen.Delanghe@lmsintl.com
Jan Anthonis – LMS International
Fabio Santos – LMS International
Herman Van der Auweraer – LMS International

Abstract :
In this paper, an integrated multi-physics approach has been developed for the simulation of switched reluctance based drivetrain systems. Two methods are presented - one concerning the NVH modeling of such a motor, while the other focuses on a multi-scale thermal model of an electric vehicle. Both methods stem from a detailed functional model of the switched reluctance motor, which is then used as the main base for the thermal and NVH modeling cases. The main objective is to present the design process of both methods and to show how such a method can be used as a vehicle integration tool. Two simulation examples are shown, one for the NVH aspects and the other for the energy management system, to illustrate the capabilities of the methods.

1. Introduction

With the electrification of road vehicles, several new design engineering challenges emerge. New components and subsystems such as battery and electric drive systems are introduced and performance parameters such as energy consumption get a new meaning because of the intrinsic range implications. The specific nature of these components and their vehicle integration requirements imposes to critically investigate the design engineering process itself and explore new tools and approaches. In the present paper, such approach is illustrated for the specific case of the design and vehicle integration of a Switched-Reluctance (SR) electric motor. Such SR-based drive systems gain interest because of their robust and low-cost designs and the absence of the need of rare earth materials. To develop such motors, it is a prerequisite to take into account from the start not only component performance specifications, but also the vehicle integration and vehicle performance requirements.

A multilevel modeling approach is proposed and illustrated for both a full electric vehicle (FEV) and a hybrid electric vehicle (HEV) integration case. The model starts from a detailed functional (1-D) motor model, the parameters of which are determined from an electromagnetic finite element model of rotor and stator at various positions. This detailed 1-D model allows quantifying torque and torque ripple, currents, efficiency and various types of losses. It forms the basis for the motor design and the development of the motor controller.

To determine requirements of the motor on vehicle level, a computationally efficient behavioral motor model is derived. This model computes the average functional characteristics such as torque, rpm and current but also the heat production and temperature distribution of the motor. It is integrated in a complete vehicle model that includes other components of the powertrain such as the battery, a combustion engine in case of a HEV, and also other energy consumers and heat producers, like HVAC, the inverter, and cabin thermal models. In this way, driving cycles and scenarios can be simulated such that a global power consumption prediction can be performed, cooling systems can be designed and typical motor operating conditions can be derived. The same detailed functional model can also be used to calculate the phase currents which, using an electromagnetic FEM model, yield the radial stator forces at each rotor position (and time step). After transformation to the frequency domain and application to a structural model, surface accelerations and hence acoustic contributions can be calculated, leading to a noise, vibration and harshness (NVH) model. The result of the thus defined modeling approach is that design parameters for the motor, the cooling system and the motor control can be linked to multiple vehicle performance parameters. The paper will focus on the workflow and critical design issues and show key simulation results. Vehicle integration validation tests will be performed as a next step but are not part of this paper which focuses on the virtual powertrain approach to design the motor and controls.

2. Introduction

2.1 THE SWITCHED RELUCTANCE MOTOR

The switched reluctance motor (SRM) is a type of synchronous machine, but with particular features - the stator windings make use of field coils, but no coil or magnetic material is present on the rotor. The motor works by energizing two opposing stator poles, generating a magnetic field. This magnetic field forces the rotation of the closest rotor poles to the position of minimum reluctance, aligning them to the stator poles. Figures 1(a) and 1(b) show the energizing and alignment of the stator and rotor poles. By energizing consecutive stator poles, continuous rotation is generated on the rotor. The SRM functionality and modeling is thoroughly explained in [1]. The switched reluctance motors are usually referred to by their number of stator and rotor poles - hence, Figures 1(a) and 1(b) represent an 8/6 SRM (8 stator poles and 6 rotor poles).

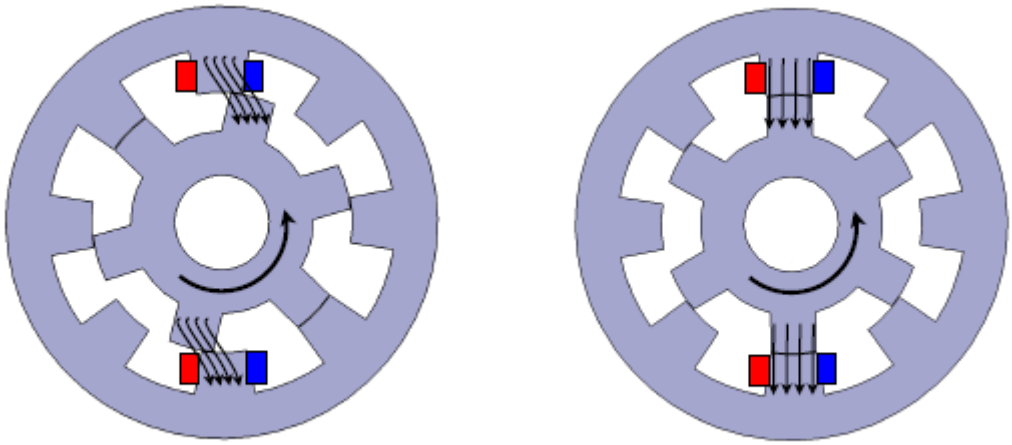

Figure 1: Switched reluctance motor functionality

The way that each phase is energized, also referred to as turn-on and turn-off angles or firing angles, is an important part of the motor activation. The proper synchronization of the phase currents with the rotor position minimizes torque ripple [2] and helps reduce current peaks and consequently copper losses. A multi-physics modeling approach was used to create a simulation model of a 12/8 SRM to be used in an integration case for both FEV and HEV systems, relating to the vehicle thermal management and NVH properties. Figure 2 shows the workflow of the modeling process, that stems from the electromagnetic motor model, that is used to create a 1D functional model. This functional model can then be used in two different ways - acoustic properties prediction or vehicle thermal model. The next sections will be dedicated to explaining in more detail the whole process.

2.1.1 Motor Functional Model Design

The switched reluctance motor is a non-linear system mainly due to the non-linear inductance profile, leading to a non-linear torque equation [3]. There are solutions available for the analytical modeling of the SRM [4], [5], but a more detailed and precise model can be obtained by the use of look-up tables containing the non-linear inductance profile and other important magnetic characteristics (on [6], there is a good comparison between linearized models, non-linear analytical models and models using look-up tables). Look-up tables gave the best results overall and for this reason they were chosen as the method to represent the 1D 12/8 SRM system.
To obtain the magnetic characteristics for this virtual model, an electromagnetic finite element model was used [7]. This model uses the stator and rotor geometry (Figure 3(a)) and material

magnetic properties, as well as the coil characteristics such as the number of wire turns, to obtain the steady state system response (Figure 3(b)), from which magnetic flux and torque can be extracted for a given rotor angular position and current. If this calculation is carried out for different rotor angles and/or currents, new flux and torque values are obtained.

This procedure can then be repeated multiple times to obtain flux and torque data for a discrete range of current and rotor position values that cover the whole operating range of the SRM [8, 9]. Figures 4(a) and 4(b) represent the torque and flux linkage (magnetic flux) data obtained from this kind of procedure - the 0◦ position represents the rotor tooth when it starts been affected by the magnetic field, while at 22.5◦ the rotor tooth is fully aligned with the stator tooth and the 45◦ position is when the rotor tooth stops being under the influence of that magnetic field. Since each phase individually has the same behavior for a given current and relative rotor position value and assuming that magnetic flux superposition is true for all cases, the look-up table data can be extracted only for a single phase and be replicated for the other phases.

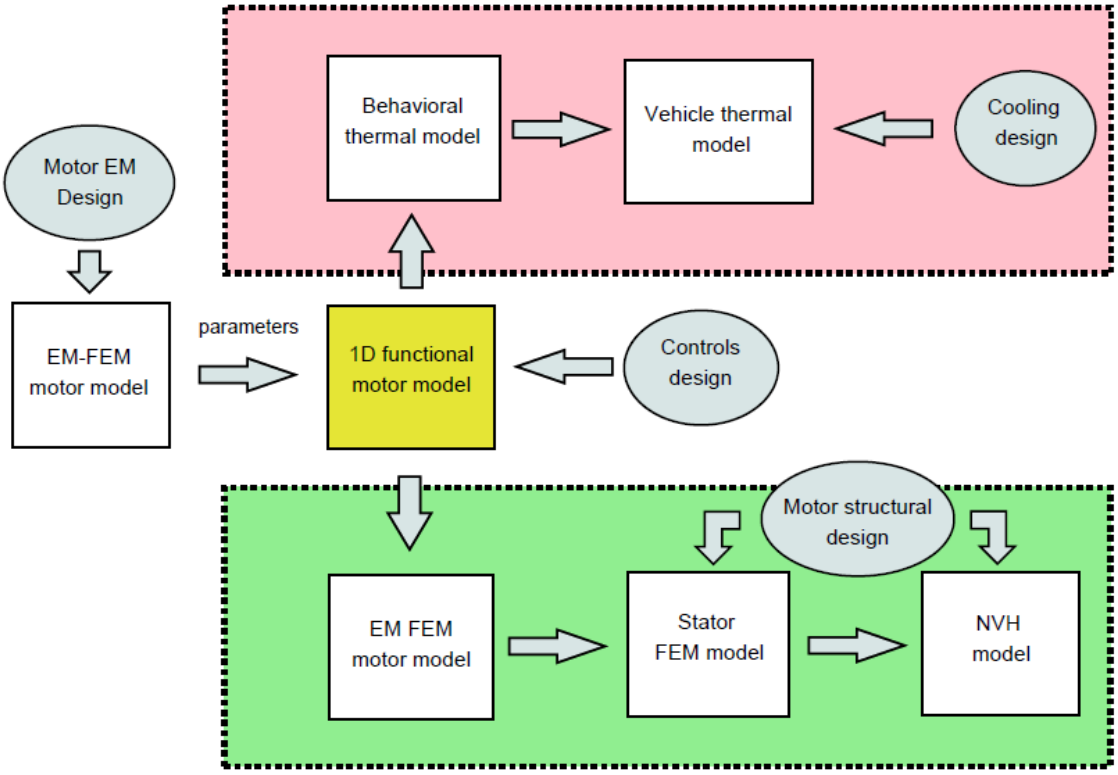

Figure 2: Multiscale SR motor model for full vehicle integration

For this paper, JMAG software is used [10] which is used to generated the look-up tables. Once the look-up tables are obtained through consecutive finite element simulations, the complete functional model can be implemented. This model has the SRM and its look-up tables, but is complemented by the possibility of adding controls, power electronics, loads, activation angles and losses model. The 1-D functional model was developed in the software LMS Imagine.Lab AMESim [11], [12]. AMESim is a 1-D multi-domain simulation software that allows for interactions between mechanical and electrical domains and is very suitable for the simulation of FEV and HEV, integrating different physical domains. Figure 5 shows the 12/8 SRM system with 3 half-bridge converters and activation angle control.

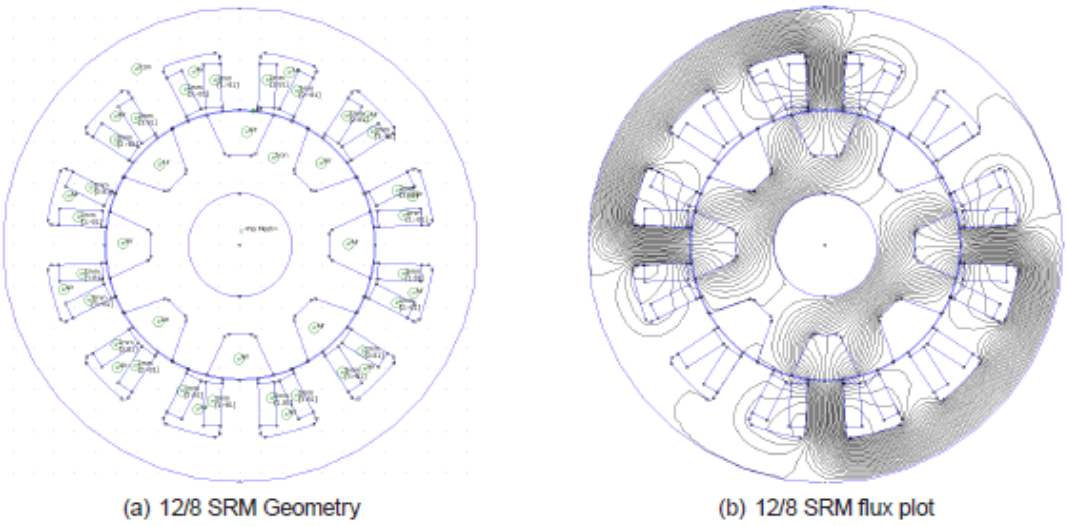

Figure 3: SRM electro-magnetic finite element modeling - (a) stator and rotor geometry; (b) magnetic flux plot

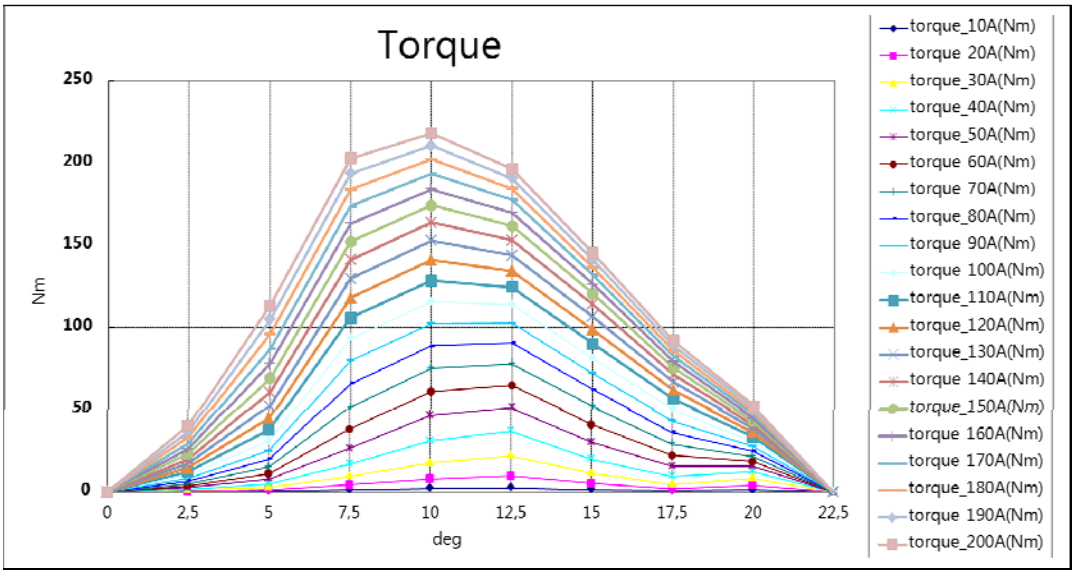

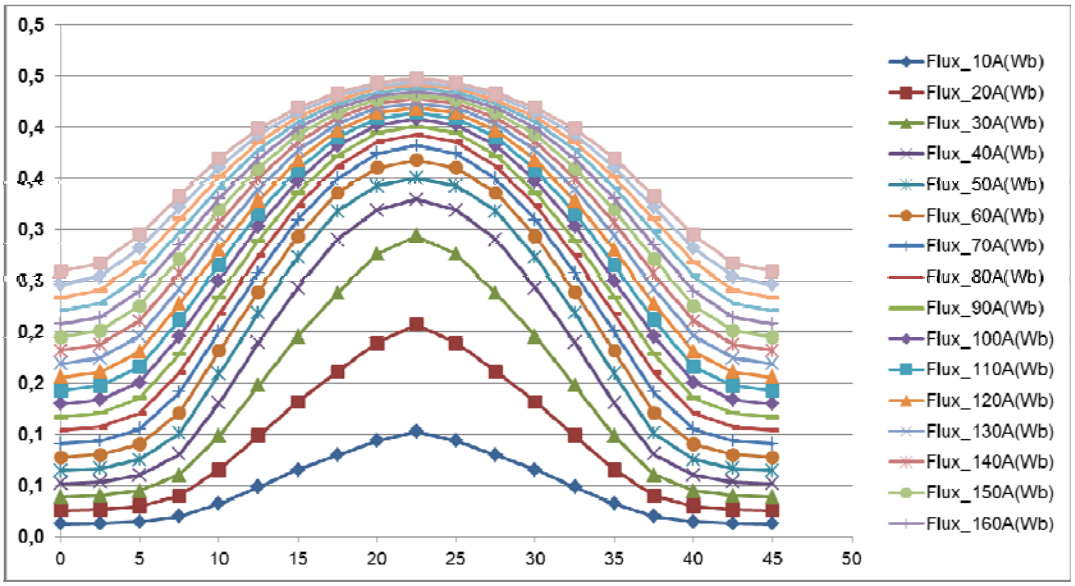

(a) Phase torque in function of rotor angle and current - the different lines represent current values going from 0 to 205 Amperes	(b) Flux linkage in function of current and rotor angle - the curves represent the phase angles ranging from 0 to 45 degrees

Figure 4: Torque and flux plots for a single phase of the 12/8 SRM calculated by JMAG

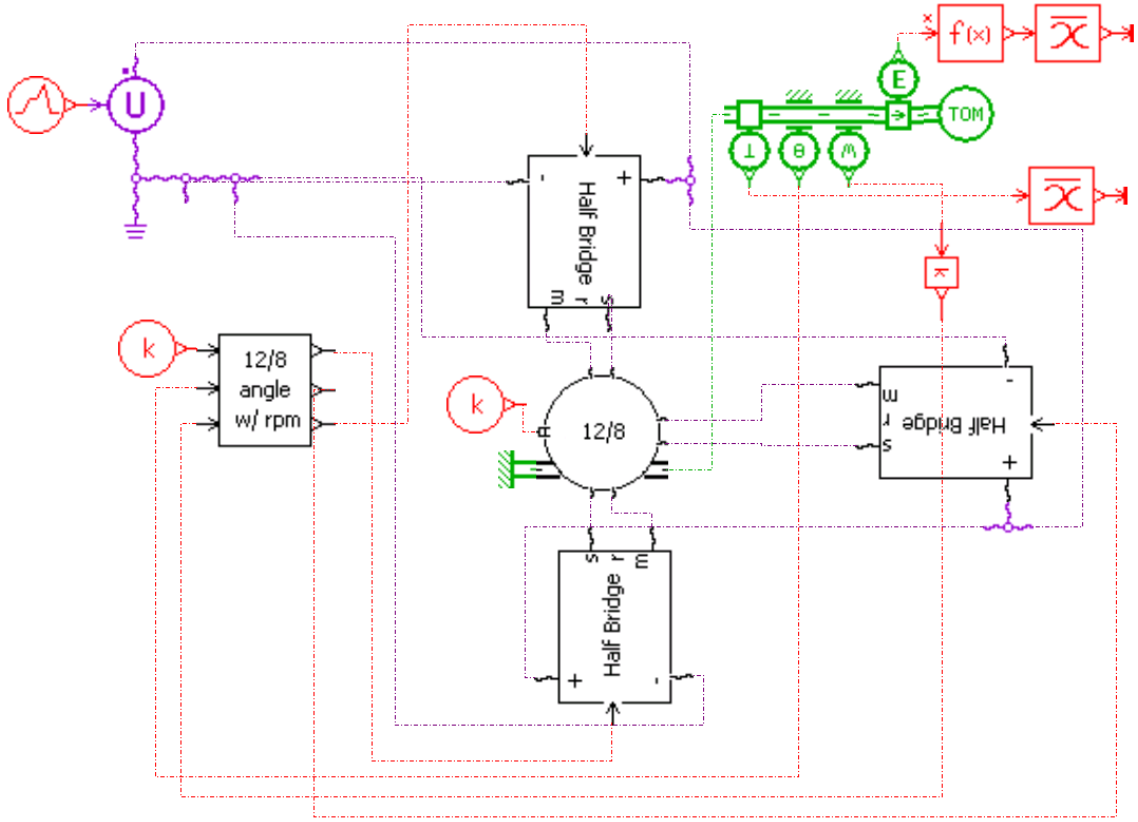

Figure 5: 1-D functional model of a 12/8 SRM with half-bridge converters and controlled firing angles from LMS Imagine.Lab

2.2 NVH Model

The acoustic analysis and noise contribution of the electric motors on FEV's and HEV's is the subject of many concerns in the automotive industry [13], [14]. For this reason, it is very important to predict the acoustic properties of the vehicle as early as possible in the design phase. The dominant cause of noise generated from the electric motors is considered to be the stator vibrations caused by radial forces [15], [16]. The radial magnetic forces in the air gap between rotor and stator teeth excite vibrations that are transferred through the structure to the external surface of the motor and through the air. Basically, the SRM noise prediction can be divided in 3 consecutive parts:

• **calculation of stator radial forces**;

• **vibration or structure-borne transmission of the forces**;

• **noise generation**.

A method was established to predict the acoustic contribution of an SRM by going through these 3 steps. By using the detailed 1-D model described in section 3.1.1, it is possible to calculate the phase currents and motor rotor position of a given working or load condition. This data can be used in JMAG to determine the magnetic forces in the air gap that act on the stator. The

magnetic forces acting on the stator teeth are surface density and volume density magnetic forces, but the latter can be neglected with respect to the surface forces [17]. This procedure can be usually done for only one full rotation, given that the motor is working on steady state conditions. The calculated forces are then divided into x and y directions and are transformed to the frequency domain.

Subsequently, the structural modes of the stator are calculated by means of the finite element method, NASTRAN in this case. Figure 6 shows some structural vibration modes of the 12/8 SRM stator. These vibration modes are used together with the magnetic forces generated previously to calculate a modal-based forced response, which consists of the surface accelerations of the stator based on the magnetic forces excitation. Finally, the calculated accelerations are the boundary conditions to be used with the FEM AML direct method, used for exterior problems.

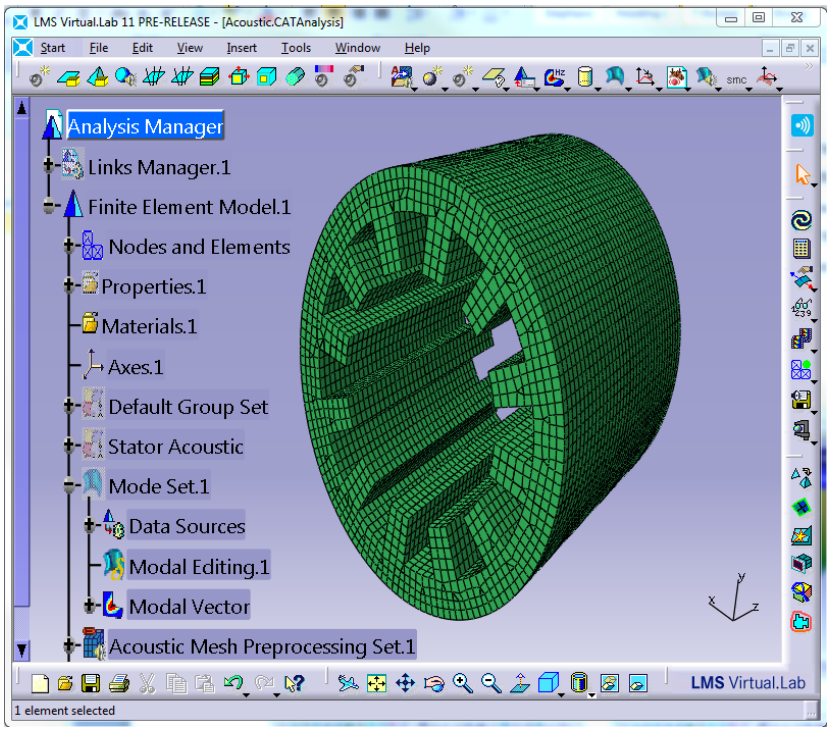

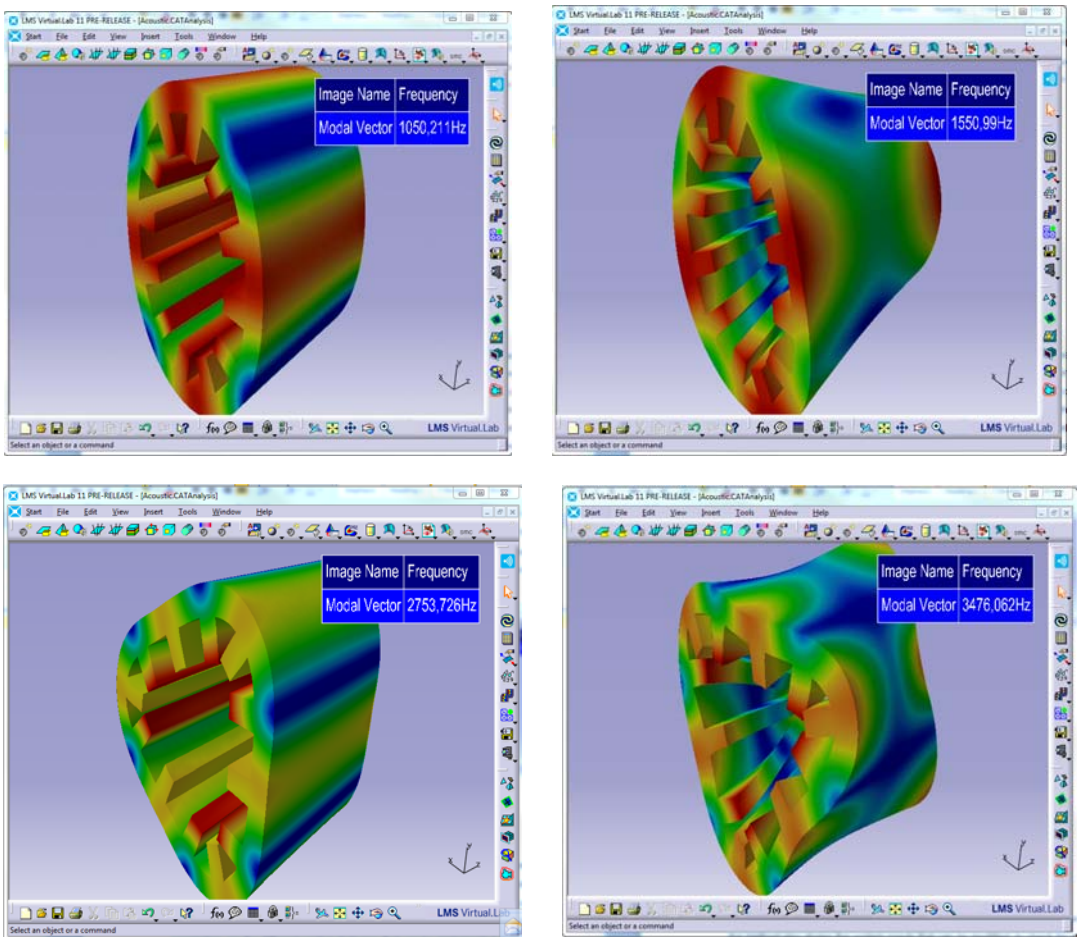

FIGURE 6: structural modes of stator

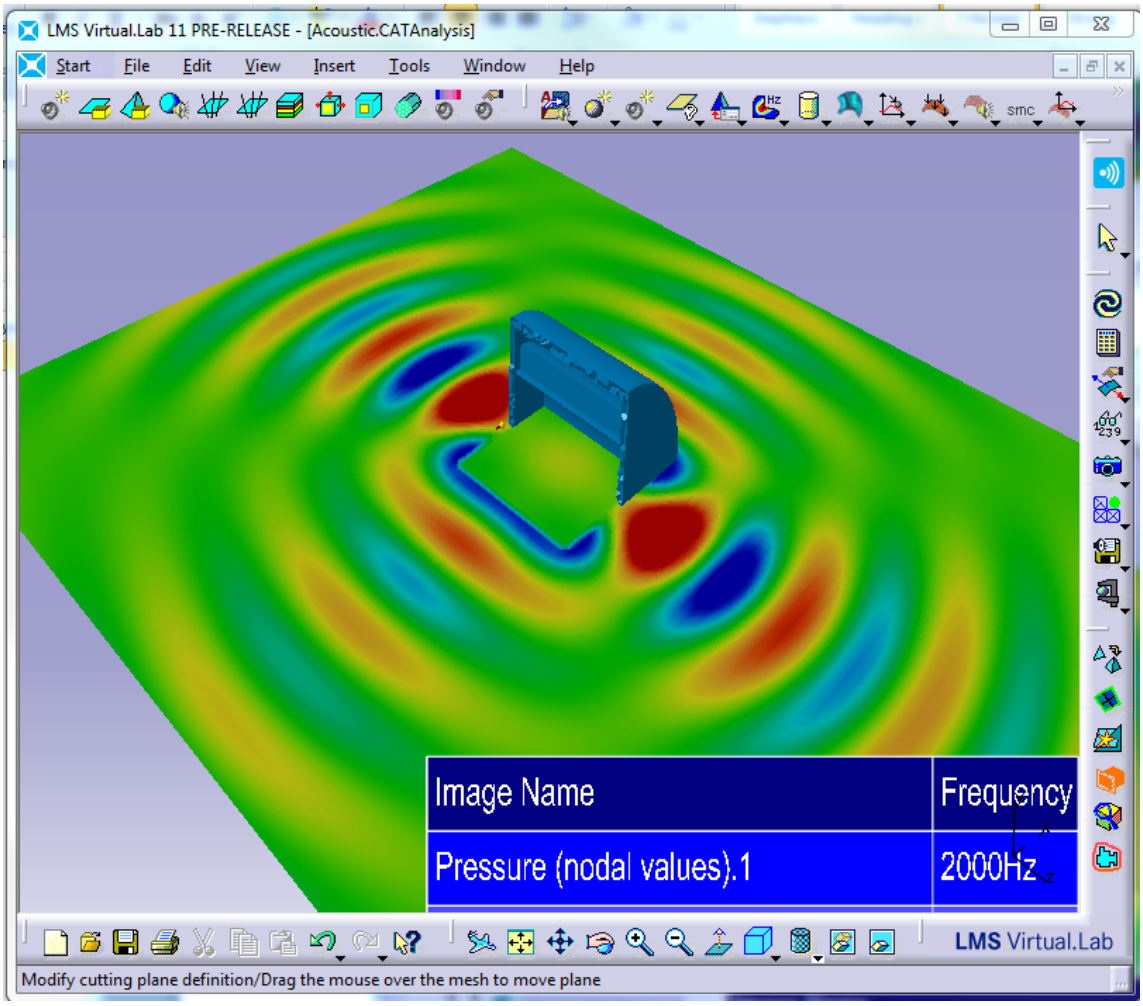

FIGURE 7: Acoustic model of the system

The whole process of the acoustic prediction methodology is shown on Figure 8. Each step of the method also shows the system inputs that can be modified, to check for improvements in the final results. In the first step, the most important inputs are the material and coil magnetic properties, as well as the stator and rotor geometry. For the 1-D simulation, the most important parameters are the different control strategies that can be implemented, together with different load conditions and/or operation cycles. The third step of the process is where the force calculations take place, and on the last part of the process, the most important inputs are the structural properties of the motor stator, which can affect directly the sound pressure levels around the motor.

System inputs: Materials Coil magnetic properties geometry	Simulation scenario's;: - Control - Load Conditions - Operation cycle	Forces on stator are calculated using JMAG	Forces from JMAG are imported into VL and vibrations and noise are calculated
2D JMAG Calculation	**1D AMESim Simulation**	**2D JMAG calculation**	**3D Noise and Vibration**

			calculation
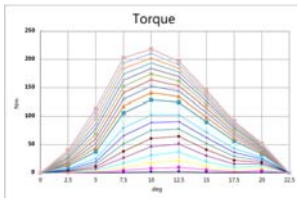	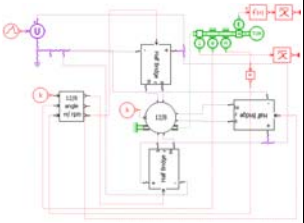	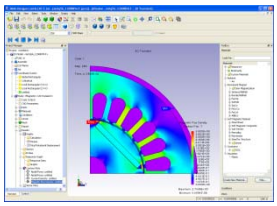	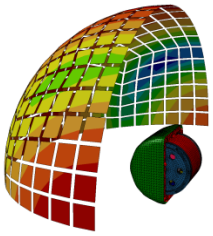

Figure 8: process view

3.3 Behavioral Motor Model and Energy Management

The investigation and simulation of the global energy consumption of the FEV's and HEV's is an important stage in the development of these vehicles [18]. By estimating the different system losses it is possible to dimension adequately the vehicle's systems, such as motor and cabin cooling or battery power consumption, based on the operating conditions [19]. Similarly, the vehicle powertrain characteristics can be evaluated before prototyping, based on suitable driving cycle scenarios [20].

To be able to obtain a computationally efficient simulation system that is able to compute the global energy flow, a simpler motor model has to be used, that is able to provide the simulation with just the necessary data needed for the losses computations. This behavioural model contains data that can be extracted from a more detailed motor model, such as the one described in section 2.1.1, or from real measurements. Three look-up tables are used in this simpler model:

• Maximum motor torque in function of input voltage, rotary velocity and temperature

• Maximum generator torque in function of input voltage, rotary velocity and temperature

• Motor losses in function of torque, rotary velocity and temperature

The tables containing the maximum motor and generator torque can easily be obtained using the detailed functional model (as in Figure 5), by running it under different conditions - rotary velocity, input voltage and temperature. Then the average torque is extracted from the system and the tables can be created. To obtain the losses table, a submodel that can compute the motor losses was created. This submodel divides the losses in 3 different types - copper losses, core losses and mechanical losses [21]. Copper losses are generated when the current goes through the coil, iron losses are related to the magnetic flux that passes through iron (stator and rotor) and mechanical losses are generated from friction. The losses table is computed in function of the motor torque and rotary velocity, as well as temperature, since it also affects energy losses, specially due to the coil resistance change with temperature.

Thereafter the 3 tables can be utilized in the SRM behavioral model that is included in a global electric vehicle system specially designed to verify the system's energy flow. The complete energy flow model of this electric vehicle is seen on Figure 9. The system, which is a global EV model, can be basically divided in 7 parts:

• Driver

• Vehicle

- ECU
- Switched reluctance motor
- SRM thermal model
- Battery
- Inverter

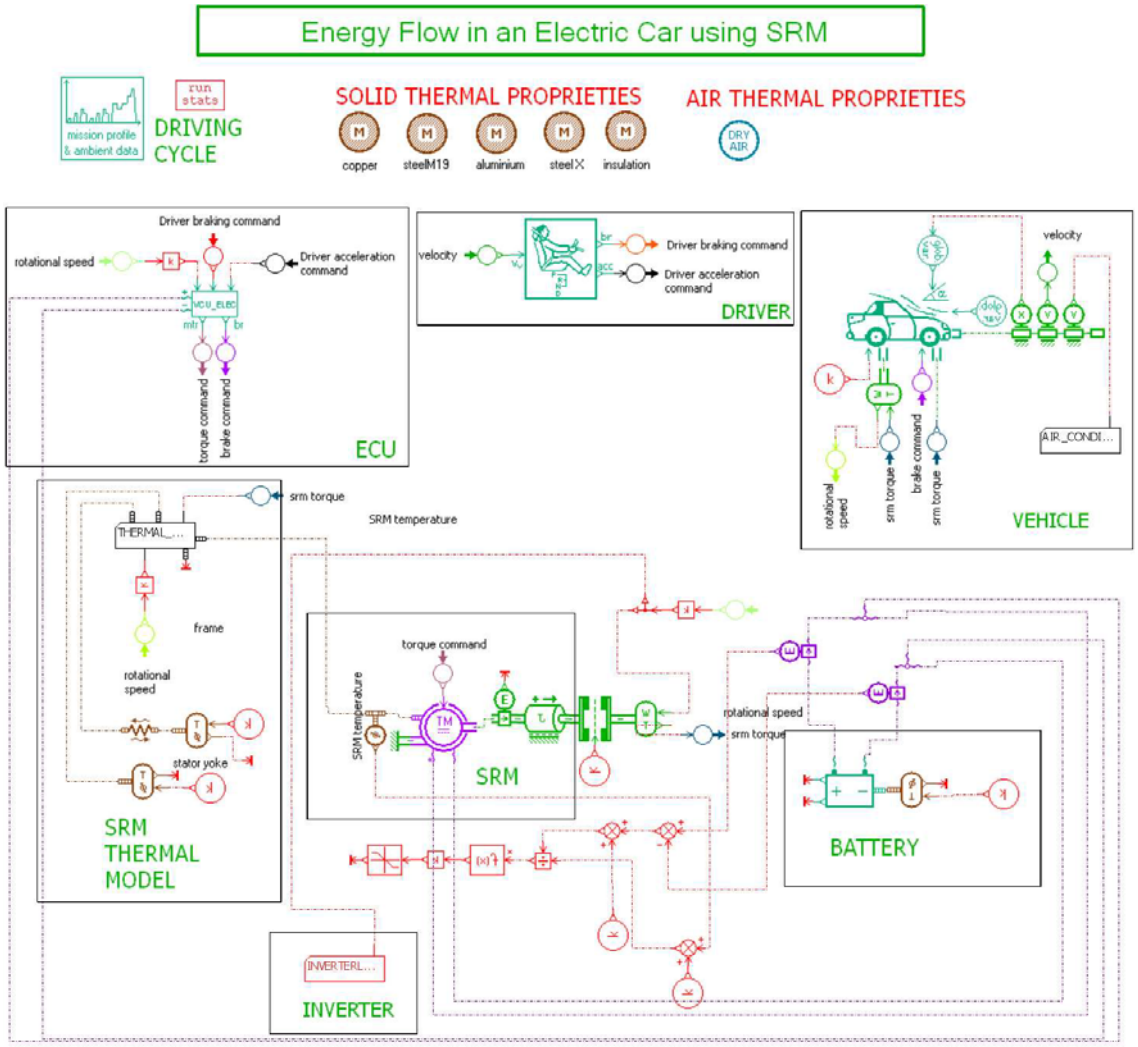

Figure 9: AMESim model of an electric vehicle with energy flow management

The Driver, ECU and Vehicle subsystems are used to simulate braking and acceleration commands, as well as simple translational dynamics for the whole vehicle, given a constant load. The Vehicle subsystem also includes an air-conditioning model that is able to regulate the cabin temperature. Benchmark driving cycles consisting of input velocities are used to simulate different operating conditions. The switched reluctance motor and its thermal subsystems - inverter, battery and the SRM itself - are used to compute the temperature and energy losses in the different component parts. To model the temperature distribution in the SRM, a lumped thermal model of the SRM was used. This model uses a thermal equivalent circuit to model the temperature distribution in the motor. The motor is divided into several thermal parts: frame, stator yoke, stator teeth, rotor core, rotor teeth, coil windings and lateral windings, axial shaft, bearings, internal air and air gap [22]. The whole thermal network is shown on Figure 10.

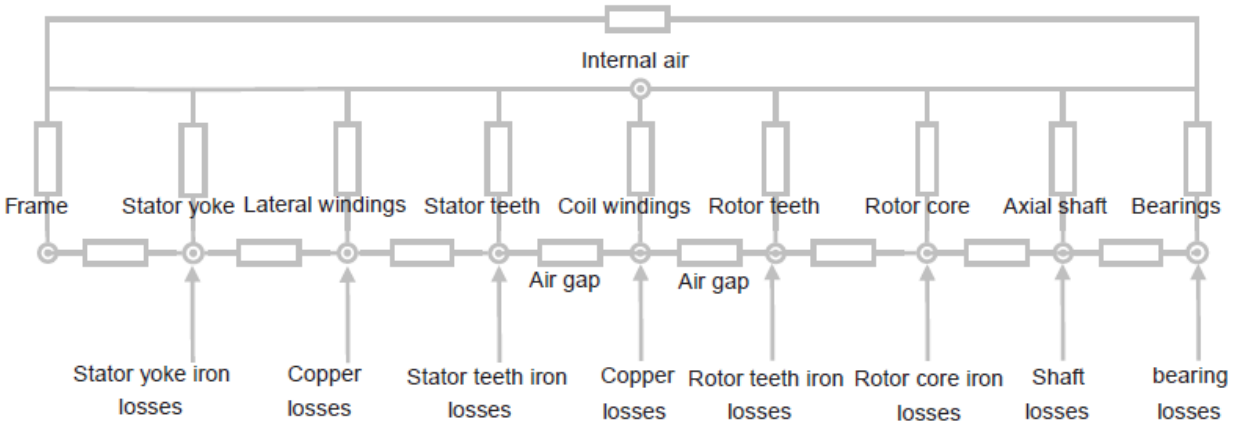

Figure 10: SRM thermal network

The thermal component of the SRM also allows for the cooling system to be connected to it. There are two inputs that are connected directly to the frame and stator yoke, in a way that a thermal network representing the cooling system can be created, based on a given geometry, and its effect on the motor temperature can be visualized on the motor itself. The inverter losses are modeled as a half-bridge with two types of components - diodes and transistors - and the losses are also divided into two types - conduction and switching losses [23]. By using the motor rotational velocity as input, the switching losses are calculated, and the conduction losses are calculated based on peak and average current values.

Losses on the battery are estimated with a model that takes into account the internal resistance of the battery, as well as the open circuit voltage. This model uses two look-up tables that represent one cell of the battery, the first table containing the open circuit voltage in function of the temperature and depth of discharge and the other containing the internal resistance in function of temperature and depth of discharge. This data can also be obtained experimentally to ensure good simulation precision.

2.4 SIMULATION EXAMPLES

Two simulations were carried out to verify both the NVH model of the SRM and the vehicle thermal model of the electric vehicle.

2.4.1 Acoustic Analysis

Following the procedure described in section 2.2, an acoustic prediction of the SRM was carried out for two working conditions, to evaluate the simulation method. The firing angles are very important in the SRM with respect to maximum and minimum current, as well as torque production and for this reason they were chosen as parameters to be investigated, to evaluate their effect on the sound pressure levels produced by the motor. The two cases chosen were: firing angles optimized to maximize torque and firing angles optimized to maximize torque and minimize mean current levels. The objective was to evaluate if, by minimizing the coil current, a significant improvement on the acoustic quality of the SRM would be seen, due to the reduction of the magnetic field amplitude generated by the coil, leading to the decrease of the forces exciting the stator teeth. The parameters used for the 1-D and 3-D simulations are shown on Table 1. To control the torque generated by the motor, a simple PI controller was used, and the chosen rotary velocity was guaranteed by attaching an auxiliary motor to the SRM shaft.

Table 1: Acoustic Simulation Specifications

Parameter	*Value*
Rotating velocity	6000 rpm
Torque	30 Nm
Minimum Frequency	200 Hz
Maximum frequency	3500 Hz

The sound prediction method used, as described in section 2.2 was the FEM method using AML for the radiation. This method allows for the use of field point meshes, that let the system's response be visualized at that specific location. On Figure 11, the sound pressure levels of the two simulation cases is shown for a planar field point mesh of 1.2m by 1.2m at 1604 Hz.
To better visualize the acoustic response over the whole frequency range, a spherical field point mesh was used to obtain the acoustic power on all points around the stator and an average value of the surrounding pressure levels is computed for each frequency. The resulting graph is shown on Figure 12, where the acoustic power responses of both simulations are shown.
The simulation results show a clear difference between the acoustic properties on the two cases. The minimization of the current has an important effect on the acoustic power response of the SRM. However, on some frequency ranges the system with current minimization has higher acoustic power levels. This happens because the current levels at that particular frequency band are higher, even though the mean current levels are lower for that case.

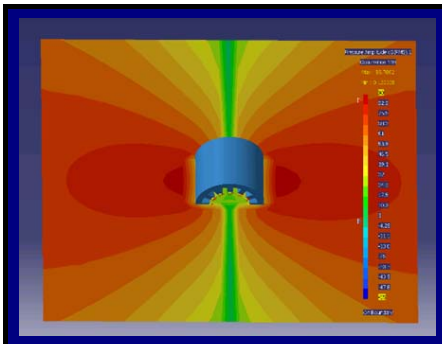

(a) Sound pressure levels for the SRM on a planar field point mesh - system with torque maximization

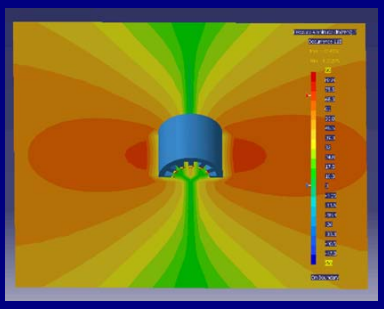

(b) Sound pressure levels for the SRM on a planar field point mesh -system with torque maximization and current minimization

Figure 11: Comparison of the sound pressure levels of the two simulation cases at 1604 Hz - (a) SRM with firing angle optimization with regards to torque (b) SRM with firing angle optimization with regards to torque and current

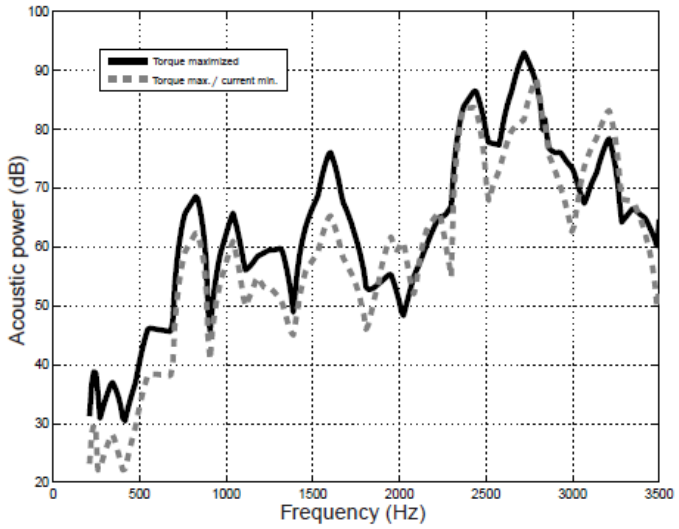

Figure 12: Comparison of the acoustic power response of a 12/8 SRM at 6000 RPM and 30 Nm torque - two firing angle strategies: (–) System response with maximized torque in respect to the firing angles (—) System response with maximized torque and minimized current with respect to the firing angles

2.4.2 Electric Vehicle Energy Management Simulation

To evaluate and test the global vehicle model, two simple cooling scenarios were used. Both scenarios consider the use of a hypothetical cooling jacket that is meant to cool the SRM frame. On the first case, the cooling fluid temperature is set as 35◦C and on the second case it was chosen as 45◦C. The objective in this case is to observe the motor temperature with respect to the cooling fluid temperatures. This sort of procedure can be very helpful on determining the optimal specifications of the cooling circuit of the motor, so that on one hand the motor temperature is kept within operational limits, and on the other hand no over-dimensioning of the cooling circuit is done, avoiding wasting too much extra energy with it.

The simulations use the New European Driving Cycle (NEDC) as the operational conditions. This driving cycle contains both an urban driving cycle and an extra-urban driving cycle, relating to city and highway driving modes, respectively, with total duration of 1180 seconds. The vehicle velocity (Km/h) in function of the total driving cycle time for the NEDC is shown on Figure 13.

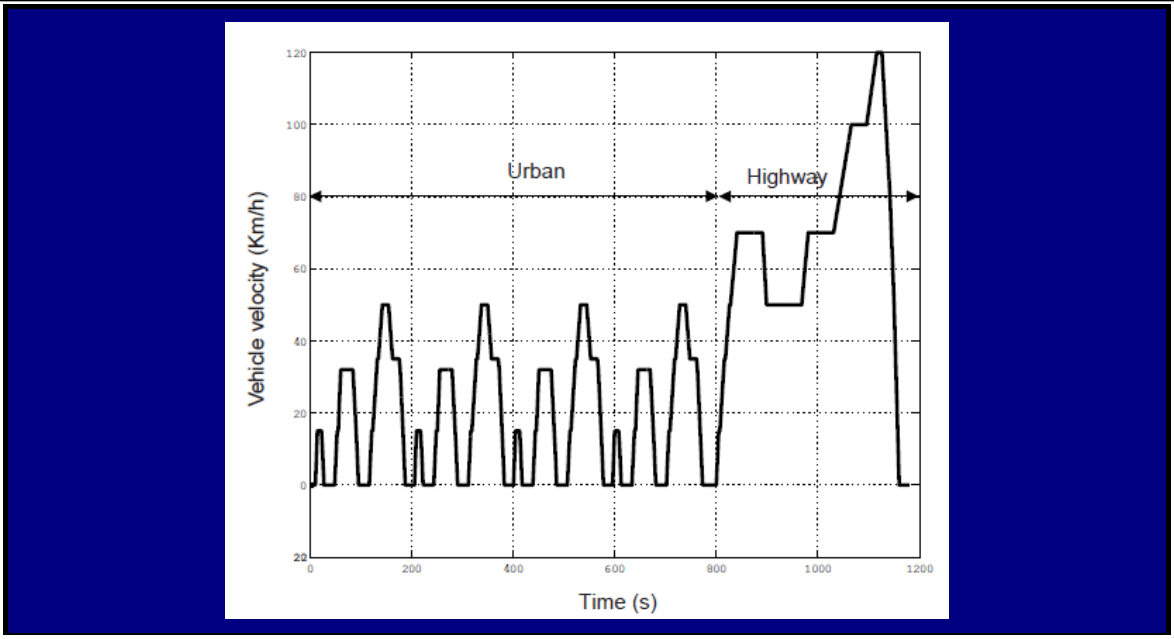

Figure 13: New European Driving Cycle used for the global electric vehicle simulation, with urban and highway cycles The main motor and system losses (total SRM losses, copper, iron and mechanical losses, battery and inverter losses), which are the same for both simulation scenarios, are shown on Figures 13(a) and 13(b).

The temperature rise in the SRM is mainly caused by the heating of the copper windings. Consequently, the windings and stator teeth are the most critical part to be monitored in the SRM. To verify the effectiveness of the cooling circuit, the temperature rise was observed on the two critical parts plus on the stator yoke, which is in direct contact with the frame and the cooling circuit. Figure 14 shows the temperature rise for both simulation scenarios - cooling fluid and jacket at 45◦C and at 35◦C Analyzing both simulation scenarios, the difference of the temperature values in the SRM parts can be clearly seen. The temperature on the coil windings is well influenced by the cooling circuit.

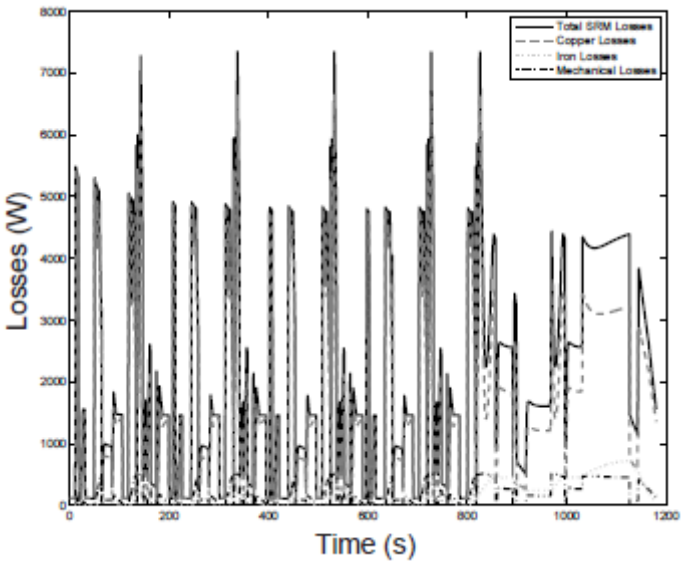

(a) Total SRM losses, copper losses, iron losses and mechanical losses for a NEDC simulation of the global vehicle system

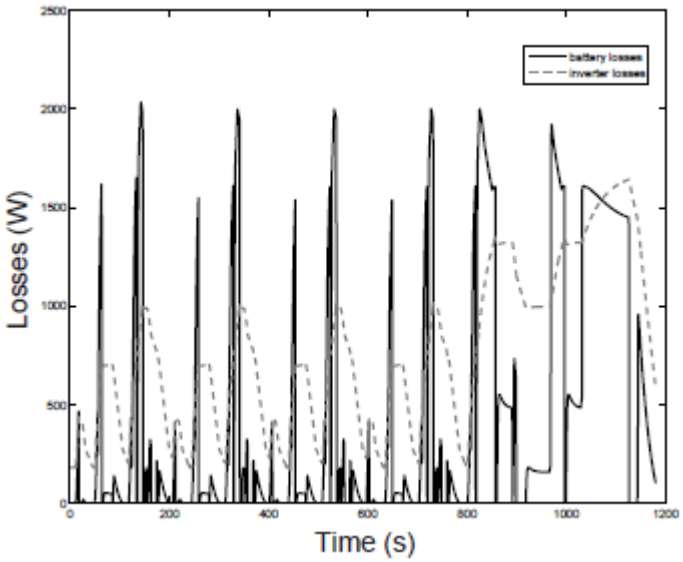

(b) Battery and inverter losses for a NEDC simulation of the global vehicle system

Figure 14: Integrated electric vehicle system losses - simulation results

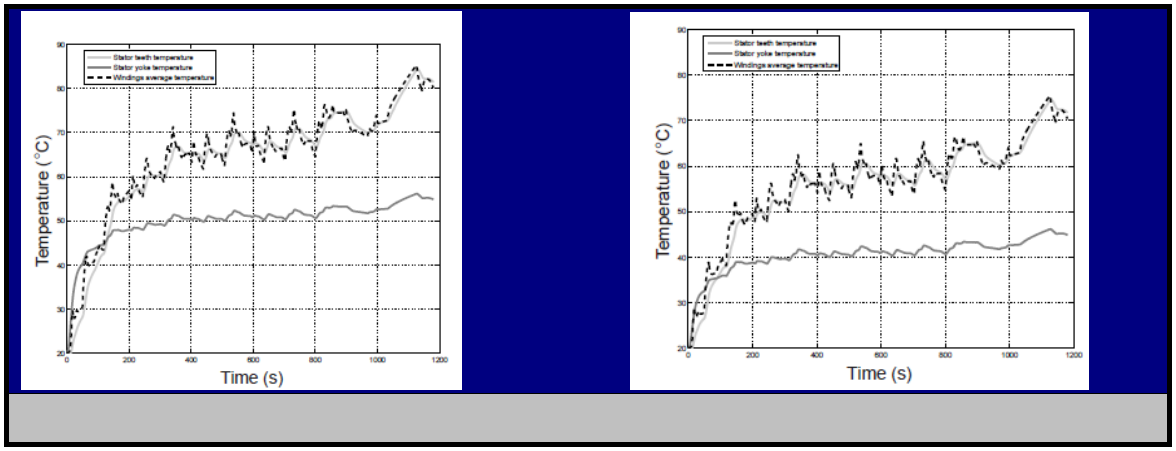

(a) Simulation with cooling fluid at 45◦C (b) Simulation with cooling fluid at 35◦C

Figure 15: Temperature rise on a NEDC cycle, analyzed at critical points of the Switched Reluctance Motor - stator yoke, stator tooth and coil windings

3 Conclusion

A detailed functional model was created by means of an integrated approach that uses magnetic finite element modeling to generate look-up tables that contain the non-linear inductance profile and magnetic torque characteristics of a 12/8 SRM. The procedure includes the use of 1-D simulations that allows for the quantification of essential parameters such as torque, phase currents and rotor position. Following the description of the SRM modeling, two modeling paths were shown - an NVH prediction approach and a global electric vehicle system to compute losses and thermal management.

The NVH modeling procedure describes the process used to compute sound pressure levels of a switched reluctance motor based on a 1-D simulation. An example was shown on how the controlling aspect of the system can affect the radiated sound. This procedure allows the

identification of the noise sources and how they affect the acoustic quality of the system. Different types of control strategies can be analyzed, as well as different load conditions, to better quantify the noise source. The structural parameters of the stator are also relevant, and can be modified to verify the benefits in the system. Overall, the method allows for a further investigation on how different system parameters, such as control strategy, current, loads, velocity, torque, structural properties, and others, affect the one specific objective, which is the acoustic property. Furthermore, trade-offs can be further investigated so that the optimal parameters can be chosen based on system specifications.

The behavioral motor model and the energy management system, in the same way as the NVH model, allow the computation of important design parameters. By using a detailed functional model to obtain look-up tables instead of just using a simple average model, more simulation precision is obtained. By extracting data from a more precise model, peak values that could otherwise go unchecked are taken into account, leading to more realistic results. Once again, the flexibility of the virtual design is the strong point. The two examples show how the motor cooling system specifications can be defined based on driving cycle simulations - this way the thermal properties of the motor can also be evaluated, such as the main source of heat and/or losses, and how the material properties affect the distribution of the energy. Moreover, the same kind of modeling can be applied to the cooling circuit system, allowing to determine the effectiveness of the system, and avoid reaching threshold temperatures or high energy loss states.

Future works on the method include the study of the trade-offs between acoustic quality optimization and energy and efficiency management. The aim is to verify how the acoustic improvements affect the efficiency of the system, and vice-versa - for instance, relating how firing angles optimized for acoustic improvement influence the performance of the motor in the electric vehicle. This sort of analysis is a very important aspect of the method, since it can allow trade-offs to be dealt with in a very early stage of design.

4 Acknowledgements

The authors would like to thank the IWT Agency for Innovation by Science and Technology for their financial support in the SRMOTIF project and Flanders' Drive for their financial support with the Electric Powertrain project.

5 References

[1] R. Krishnan. *Switched Reluctance Motor Drives: Modeling, Simulation*. CRC Press, 2001.

[2] C. Mademlis and I. Kioskeridis. Gain-scheduling regulator for high-performance position control of switched reluctance motor drives. *Industrial Electronics, IEEE Transactions on*, 57(9):2922–2931, 2010.

[3] S.M. Lukic and A. Emadi. State-switching control technique for switched reluctance motor drives: Theory and implementation. *Industrial Electronics, IEEE Transactions on*, 57(9):2932–2938, 2010.

[4] W. Ding and D. Liang. A fast analytical model for an integrated switched reluctance starter/generator. *Energy Conversion, IEEE Transactions on*, 25(4):948–956, 2010.

[5] E. Padurariu, L. Somesan, I.A. Viorel, C.S. Martis, and O. Cornea. Switched reluctance motor analytical models, comparative analysis. In *Optimization of Electrical and Electronic Equipment (OPTIM), 12th International Conferenceon*, pages 285–290. IEEE, 2010.

[6] F. Soares and PJ Costa Branco. Simulation of a 6/4 switched reluctance motor based on matlab/simulink environment. *Aerospace and Electronic Systems, IEEE Transactions on*, 37(3):989–1009, 2001.12

[7] K. Mhatli and B. Ben Salah. Improved modeling of switched reluctance motor including mutual and saturation effects. In *MELECON- 15th IEEE Mediterranean Electrotechnical Conference*, pages 1470–1475. IEEE, 2010.

[8] L. Chang. Modelling of switched reluctance motors. In *Electrical and Computer Engineering, 1997. IEEE 1997 Canadian Conference on*, volume 2, pages 866–869. IEEE, 1997.

[9] N.H. Fuengwarodsakul, R.W. De Doncker, and RB Inderka. Simulation model of a switched reluctance drive in 42 v application. In *Industrial Electronics Society, 2003. IECON'03. The 29th Annual Conference of the IEEE*, volume 3, pages 2871–2876. IEEE, 2003.

[10] H. Kuss, T. Wichert, and B. Szvmanski. Design of a high speed switched reluctance motor for spindle drive. In *Compatibility in Power Electronics, 2007. CPE'07*, pages 1–5. IEEE, 2007.

[11] R. Meillier, T. Rozier, A. Brizard, and D. Almer. Optimization of vehicle energy management through multi-domain system simulation. In *Transport Research Arena Europe*, 2010.

[12] L. Broglia, M. Ponchant, and R. Meillier. Balancing vehicle energy performance with drivability and thermal comfort: benefits of a multi-domain system simulation approach in the case of an electric-hybrid vehicle. In *25th World Electric Vehicle Symposium and Exposition*, 2009.

[13] J. Florentin, F. Durieux, Y. Kuriyama, T. Yamamoto, M. DeBruin, S. Jordan, J. Han, G. Barber, Q. Zou, X. Sun, et al. Electric motor noise in a lightweight steel vehicle. *Analysis*, 1:1062, 2011.

[14] O. Ilsen, N. Vaninbroukx, B. Van Hooreweder, P. Sas, S. Faid, J. Anthonis, and P. Aarnoutse. Analysis of radiated noise in electric vehicles with a switched reluctance traction motor. In *8th International Automotive Congress*, 2011.

[15] J.O. Fiedler, K.A. Kasper, and R.W. De Doncker. Calculation of the acoustic noise spectrum of srm using modal superposition. *Industrial Electronics, IEEE Transactions on*, 7(9):2939–2945, 2010.

[16] W. Cai, P. Pillay, Z. Tang, and A.M. Omekanda. Low-vibration design of switched reluctance motors for automotive applications using modal analysis. *Industry Applications, IEEE Transactions on*, 39(4):971–977, 2003.

[17] M. van der Giet, E. Lange, DAP Correa, IE Chabu, SI Nabeta, and K. Hameyer. Acoustic simulation of a special switched reluctance drive by means of field–circuit coupling and multiphysics simulation. *Industrial Electronics, IEEE Transactions on*, 57(9):2946–2953, 2010.

[18] V.P. Atluri, K. Koprubasi, and N.D. Brinkman. Analytical evaluation of propulsion system architectures for future urban vehicles. In *Advanced Hybrid vehicle Powertrains*, 2011.

[19] CC Chan, A. Bouscayrol, and K. Chen. Electric, hybrid, and fuel-cell vehicles: architectures and modeling. *Vehicular Technology, IEEE Transactions on*, 59(2):589–598, 2010.

[20] M. Woon, X. Lin, A. Ivanco, A. Moskalik, C. Gray, and Z.S. Filipi. Energy management options for an electric vehicle with hydraulic regeneration system. In *Advanced Hybrid vehicle Powertrains*, 2011.

[21] S. Shoujun, L. Weiguo, D. Peitsch, and U. Schaefer. Detailed design of a high speed switched reluctance starter/generator for more/all electric aircraft. *Chinese Journal of Aeronautics*, 23(2):216–226, 2010.

[22] H. Rouhani, J. Faiz, and C. Lucas. Lumped thermal model for switched reluctance motor applied to mechanical design optimization. *Mathematical and computer modelling*, 45(5-6):625–638, 2007.

[23] MH Bierhoff and FW Fuchs. Semiconductor losses in voltage source and current source igbt converters based on analytical derivation. In *Power Electronics Specialists Conference, 2004. PESC 04. 2004 IEEE 35th Annual*, volume 4, pages 2836–2842. IEEE, 2004.

6 Responsibility notice

The author(s) is (are) the only responsible for the printed material included in this paper